Comparison Between the Audible Noises Generated from Single Corona Source Under DC and AC Corona Discharge

Xuebao Li, *Student Member, IEEE*, Xiang Cui, *Senior Member, IEEE*, Tiebing Lu, Donglai Wang, Wenzuo Ma, and Xingming Bian

***Abstract*—The corona-generated audible noise (AN) factor is an important consideration in the design and operation of ultra-high voltage direct current (DC) and alternate current (AC) transmission lines. Due to the differences in discharge process and corona-generated space charges between the DC and AC corona discharge, the audible noise from DC and AC corona has different characteristics. This paper conducts a series of experiments by measuring the time-domain waveforms of the audible noise from a single corona source under DC and AC voltage. Sound pressure pulses are extracted from a correlation analysis, and then a detailed comparison of the basic characteristics of DC and AC corona-generated AN in time-domain and frequency spectrum is given. Results from this paper stand to contribute to an explanation of existing results in AN measurement and analysis from DC and AC transmission lines.**

***Index Terms*—AC corona, audible noise, DC corona, single corona source, time-domain measurement.**

I. Introduction

THE corona-generated audible noise (AN) has emerged as an important design factor for transmission lines, particularly since the introduction of transmission voltages of 500 kV and above. The AN from corona discharge is generally lower than other environment noise, but the frequency spectrum covers a much wider band. Therefore, the criteria of public perception and acceptance of the corona-generated AN are different from those of other environmental noises [1], [2]. Due to the higher operating voltage requirements of ultra-high voltage direct current (DC) and alternate current (AC) transmission lines, corona-generated AN has become an important topic of research [3]–[11]. However, the physical mechanism and intrinsic characteristics of AN under DC and AC corona discharge to date has received little attention.

Research thus far on AN from DC corona discharge has been primarily experimental, with characteristics and empirical formulas proposed by many scholars [3]–[5]. For example, BPA (Bonneville Power Administration), IREQ (Hydro Quebec Institute of Research), ENEL (Ente National per L'Energia), and CRIEPI (Central Research Institute of Electric Power Industry), all have proposed empirical formulas for predicting AN from DC transmission lines based on long-term noise measurement through corona cage and actual transmission lines. Ianna, Wilson, and Bosack [6] conducted investigations on the frequency spectrum characteristics of AN. Their results show that the AN caused by DC corona discharge covers a wide range of frequencies and is highly dependent on corona current pulses. In [12] AN from corona discharge is seen to have pulse characteristics. Recently, the authors of this paper used the time-domain measurement method to further analyze the pulse and correlation characteristics between sound pressure pulses and corona discharge [13], [14].

Theoretical studies on DC corona-generated audible noise are relatively sparse. Bastin provides a review of results and basic principles related to the production of sound waves produced by electrical discharge [15]. In [16], Bequin, Montembault, and Herzog employ the principle as well as establish a model of negative point-to-plane corona loudspeaker [16]. However, due to differences in operating principles between the corona loudspeaker and DC transmission line corona, the model cannot be used to calculate AN from transmission lines.

A few experimental and theoretical investigations of AN from AC corona discharge have been conducted using corona cages, test lines, and actual transmission lines [7]–[11]. Statistical analysis of the long-term measured data from AC transmission lines has also yielded interesting characteristics and empirical formulas. The spectral characteristics of AN from metallic protrusions, for example, are given in [6]. Sforzini *et al.* conducted experiments in an anechoic chamber and obtained the frequency spectrum and sound pressure level (SPL) characteristics from different conductors [9]. The broadband noise and tonal noise for the AN from AC corona can be clearly identified in their investigation. Recently, Straumann presented the mechanism and calculation model of the tonal noise from AC transmission lines [17], [18]. The results in this work promote our understanding of the generation mechanism of the tonal noise; however, the model used cannot be used to calculate all components of AN from AC corona discharge.

Overall, due to the complex mechanism of corona-generated AN, there are no accurate models for calculating the AN from DC and AC transmission lines. Instead, their random nature

Manuscript received April 23, 2015; revised August 5, 2015; accepted August 22, 2015. Date of publication September 30, 2015; date of current version August 30, 2015. This work was supported by National Basic Research Program of China (973 Program) under Grant 2011CB209402.

The authors are with the State Key Laboratory of Alternate Electrical Power System with Renewable Energy Sources, North China Electric Power University, Beijing 102206, China (e-mail: lxb08357x@ncepu.edu.cn, x.cui@ncepu.edu.cn, tiebinglu@ncepu.edu.cn).

Digital Object Identifier 10.17775/CSEEJPES.2015.00031

and intrinsic characteristics are being identified through obtained time-domain waveforms. At present, experimental investigations that use the time-domain measurement for corona-generated AN are likely the most effective methods for obtaining the characteristics and for establishing a predictive method for corona-generated AN. Moreover, the de-noising method in time-domain is seen as effective in removing the background noise.

Thus far, the time-domain measurement method has not been widely used in the measurement of corona-generated AN, especially in AC corona-generated AN. The authors of this paper have generated basic results on AN from DC and AC corona [19], but the detailed characteristics of the audible noise pulses in time-domain and frequency spectrum have not yet been investigated.

In this paper, the time-domain waveforms of the AN caused by DC and AC corona discharge on a single corona source are obtained. Based on a correlation analysis and the pulse characteristics, the sound pressure pulses are extracted and the background noise is removed successfully. Then, the detailed characteristics of sound pressure pulses from DC and AC corona are compared and analyzed. Qualitative explanations for the differences between the AN from DC and AC corona discharge are also provided. The results in this paper are expected to provide insights into the intrinsic characteristics and generation mechanism of AN from DC and AC transmission lines.

II. Experiment Setup and Measurement

In this paper, the time-domain method is used to measure the AN. The measurement system consists of a microphone, amplifier, data acquisition card, and computer, as shown in Fig. 1. The microphone used in the experiments has a typical frequency range of 10 Hz to 20 kHz. The amplifier is used to supply the polarized voltage to the microphone, and to provide the 20 dB amplification to the output signal of the microphone. The data acquisition card typed as TiePie has two channels and the maximum sampling rate is 500 MS/s. In the experiments, the time-domain waveforms of the AN caused by DC and AC corona discharge on a single corona are recorded through one channel of the data acquisition card. The other channel is used to record the applied voltage on the conductor, which is measured through a resistance capacitance divider with voltage ratio of 1000: 1. The sampling rate is set as 200 kS/s.

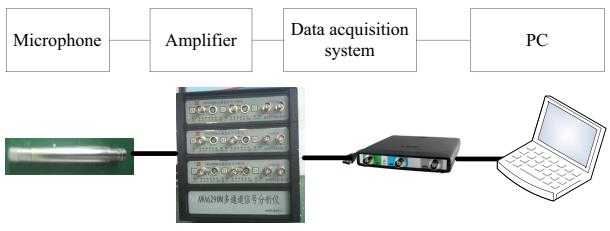

Fig. 1. Time-domain measurement system for the AN.

The structure of the corona cage is the same as that in previous work [13], [14]. The experiment arrangement is shown in Fig. 2, which is similar to that in [19]. The single corona source shown in Fig. 2(b) was simulated by a metal sphere with a diameter of 2.5 mm protruding from the conductor. The microphone is placed 0.8 m away from the corona source in a horizontal direction. The height of the microphone is same as the conductor and the microphone, directly facing the corona source. The DC and AC high voltage source are applied on the conductor, respectively. The temperature and relative humidity is set at 18.3°C and 17%, respectively.

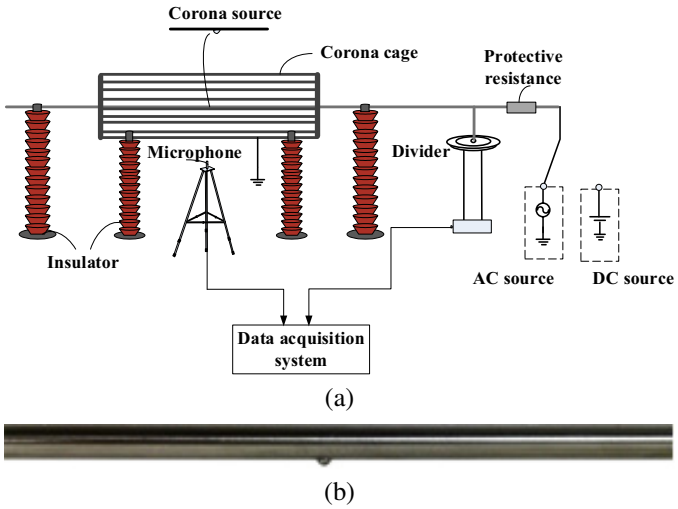

Fig. 2. Sketch figure of the experiment arrangement and the corona source. (a) Experiment arrangement. (b) Conductor with corona source.

III. Results and Analysis

A. Basic Characteristics of AN Waveforms

When the corona source is in the corona, the measured waveforms of AN under DC and AC voltages are shown in Fig. 3. For the AN from AC voltage, the waveforms of the applied AC voltage are also given in Fig. 3(c) and Fig. 3(d) to show the relationship between the sound pressure pulses and AC voltage. It should be pointed out that the sound pressure pulses in Fig. 3(c) and Fig. 3(d) have been shifted in time-domain according to the propagation time from the corona source to the microphone. The waveforms of corona-generated AN from both DC and AC corona discharge consist of a series of random sound pressure pulses with bipolar properties. The pulses from the DC positive corona consist of a series of pulse trains with large randomness, and show large pulse amplitudes and less pulse numbers. For the sound pressure pulses from DC negative corona discharge, the pulse amplitudes are smaller, with relatively fewer fluctuations, and denser pulses.

However, it can be seen from Fig. 3(c) and Fig. 3(d) that the sound pressure pulses caused by AC corona discharge are different from those in the DC corona cases. Due to the periodic change of AC voltage, the sound pulses only exist near the peak values of the positive and negative half cycle. When the AC voltage is low (at 28.85 kV rms in Fig. 3(c)), the pulses only exist at negative half cycle. As the applied voltage is further increased, large irregular pulses in positive half cycle can be detected, and the pulse number is far less. Furthermore, the pulses in negative half cycle turn much tenser

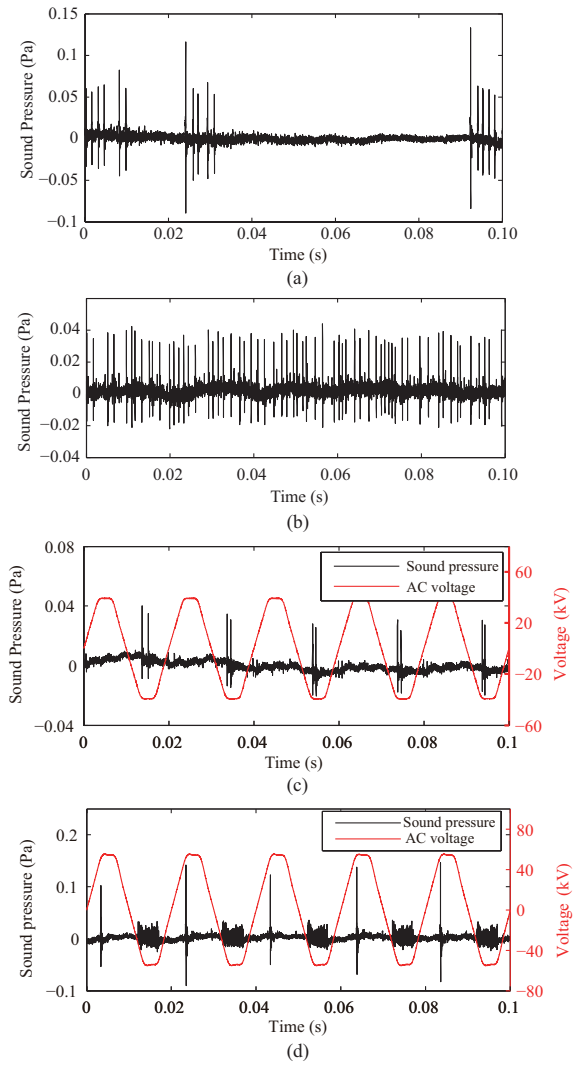

Fig. 3. Waveforms of the AN from AC and DC corona discharge. (a) +56 kV. (b) −48 kV. (c) 28.85 kV rms. (d) 40.05 kV rms.

with the increase of voltage. Fig. 3(d) shows the sound pulses from positive point type discharge as well as negative point discharge occurring during alternate half cycles.

In fact, our pervious study in [14] has shown that the sound pressure pulse and corona current pulse have one-to-one relationship in time-domain. So, the above features of the sound pressure pulses are similar to those found in the corona current pulses in early works [20]–[22].

B. Extraction of Sound Pressure Pulses and De-noising

The measured waveforms in Fig. 3 show that the background noise from ambient noise and the measurement system may introduce fluctuations of the waveforms, and thus removing the background noise may ensure further accurate analysis of the corona-generated AN.

Removal of the background noise should focus on two aspects, namely, the non-pulse region and the offset of the sound pressure pulse. In this paper, the correlation analysis was employed for extracting the sound pressure pulses, which was the key point in the de-noising process. As for the offset caused by the background noise, it can be removed according to the basic characteristics of the sound pressure pulse from a single corona source.

Based on our earlier study, the typical waveform of single sound pressure pulse can be expressed as a segmented double exponential function [13]. The normalization expression of the typical waveform (the base waveform) can be expressed as in (1); the waveform is shown in Fig. 4.

$$p_{\mathrm{b}}(t)=\begin{cases}K_1\left(\mathrm{e}^{-\alpha_1(-t+t_{\mathrm{p0}})}-\mathrm{e}^{-\beta_1(-t+t_{\mathrm{p0}})}\right) & 0<t\le t_{\mathrm{p0}}\\ K_2\left(\mathrm{e}^{-\alpha_2(t-t_{\mathrm{p0}})}-\mathrm{e}^{-\beta_2(t-t_{\mathrm{p0}})}\right) & t_{\mathrm{p0}}\le t<t_{\mathrm{d}}\end{cases} \tag{1}$$

where K_1, K_2, α_1, α_2, β_1 and β_2 are fitting parameters, t_{p0} is the zero-crossing point of the positive sound pressure part, and t_{d} is the duration time of the sound pressure pulse.

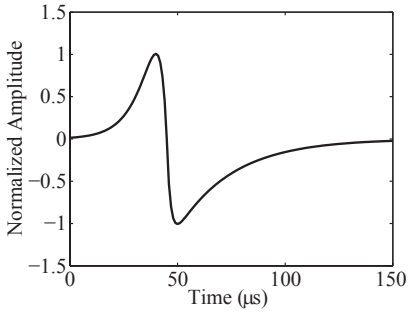

Fig. 4. Normalization waveform of the typical waveform.

The correlation function between the measured waveform of AN $n_1(t)$ and the extended base waveform $n_2(t)$, which is padded with trailing zeros to the length of $n_1(t)$, can be expressed as

$$r_{12}(t)=\int_{-\infty}^{+\infty} n_1(\tau)n_2(t-\tau)\mathrm{d}\tau \tag{2}$$

where $r_{12}(t)$ is the correlation function, and τ is the integration variable. Due to similar pulse characteristics of measured sound pressure pulses and base waveform, the sound pressure pulses will locate at the regions of the extremal points of the $r_{12}(t)$. By finding the extremal points of $r_{12}(t)$, the sound pressure pulses can be found, and then the background noise at non-pulse region can be removed by setting non-pulse signals as zeros.

The single corona source in the experiment can be treated as a point sound source with the generation of a spherical sound wave. The sound pressure at a given position satisfies the (3) in theory [23].

$$\int_{-\infty}^{+\infty} p\mathrm{d}t=0. \tag{3}$$

Therefore, the integration at each sound pressure pulse can be treated as the approximate offset from background noise. Through subtracting the corresponding offset from each sound pressure pulse, the influence of the background noise is completely removed.

Based on the above method, the de-noised waveforms for the waveforms in Fig. 3(a) to Fig. 3(d) can be shown in Fig. 5, which shows that the background noise can be successfully

removed. The analysis in the sections that follows all depends on the de-noised waveforms.

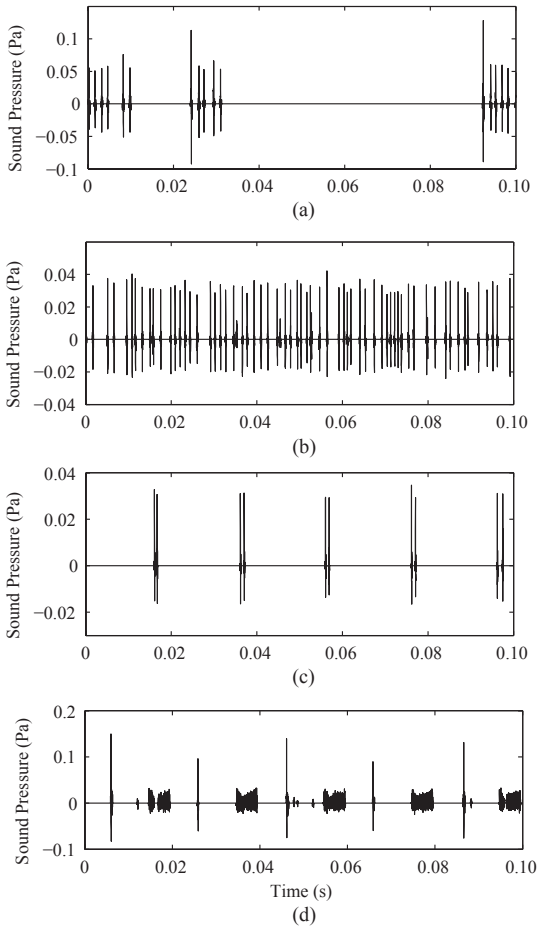

Fig. 5. De-noised waveforms of the waveforms of AN in Fig. 3. (a) +56 kV. (b) −48 kV. (c) 28.85 kV rms. (d) 40.05 kV rms.

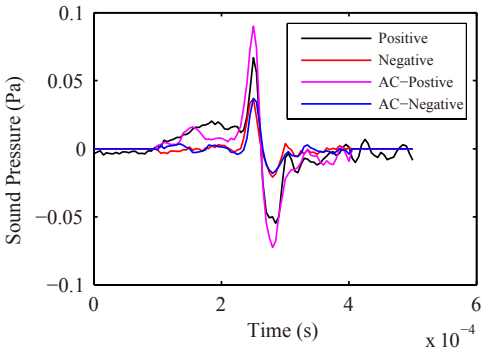

Fig. 6. Single sound pressure pulses from positive, negative, AC positive half cycle and AC negative half cycle.

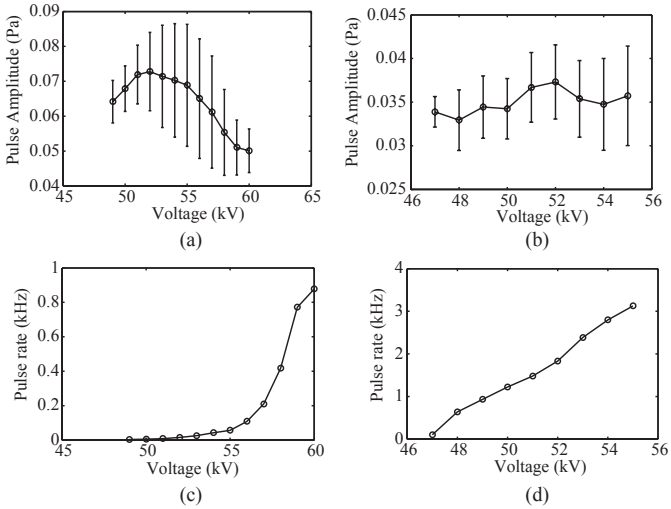

Fig. 7. Pulse amplitude and pulse rate from positive and negative corona discharge. (a) Pulse amplitude from positive corona. (b) Pulse amplitude from negative. (c) Pulse rate from positive corona. (d) Pulse rate from negative corona.

C. Characteristics of Sound Pressure Pulses

A single sound pressure pulse under DC positive, DC negative, AC positive half cycle, and AC negative half cycle are shown in Fig. 6. Each single sound pressure pulse is just one among the measured sound pressure pulse trains in Fig. 3. The amplitudes of the selected sound pressure pulses reflect the average level of the sound pressure pulse. It can be seen from the Fig. 6 that the amplitude from DC positive corona discharge is about 2 times larger than that from DC negative corona discharge. The duration time of the sound pressure pulse from DC positive corona discharge is larger than that from DC negative corona discharge. As for the AC case, a similar phenomenon can be found for sound pressure pulse from the AC positive half cycle and AC negative half cycle. In the case of the single sound pressure pulse, the pulse amplitude from AC positive half cycle seems to be larger than that from the DC positive corona discharge. Finally, the difference between the sound pressure pulse from the DC negative corona and the AC negative half cycle is likely to be minimal.

Fig. 7 shows the statistical results of the pulse amplitude and pulse rate from DC positive and negative corona discharges varying with the absolute value of the applied voltage. The voltages were resized from the onset of corona. When the resizing takes place with fierce corona, the sound pressure pulses start to appear at the corona onset. Thus, at the point of the fierce corona, the sound pressure pulses are dense. Both of the pulse amplitudes from DC positive and negative corona discharge are of a random nature, but the fluctuations of DC negative corona-generated sound pressure pulses are relatively small. The average amplitude of sound pressure pulse for the positive corona is larger than that of the negative corona. In addition, the average amplitude for DC negative corona-generated pulse changes slightly with the applied voltage, while the average amplitude for positive corona-generated pulse first increases slightly and then decreases with the applied voltage. The onset voltage of the DC positive corona is higher than that of the DC negative corona.

As shown in Fig. 7(c) and Fig. 7(d), the pulse rate for the DC positive corona increases exponentially with the applied voltage, while the pulse rate for the DC negative corona increases linearly with the applied voltage, which is similar to the results of the corona current [21], [22]. The pulse rate for DC positive corona is lower compared with that for the

DC negative corona.

Due to the alternating polarity and varied voltage over time, the sound pressure pulses from AC corona have different characteristics from those observed in the DC corona case. Fig. 8 shows the phase spectrum figures of the sound pressure pulse amplitudes at different AC voltages. The vertical coordinate is the pulse amplitude, and the horizontal coordinate is the phase angle [24]. It should be mentioned that the sinusoidal waveform in Fig. 8 gives only the phase reference. The discrete points of pulse amplitudes are the statistical results in 30 cycles.

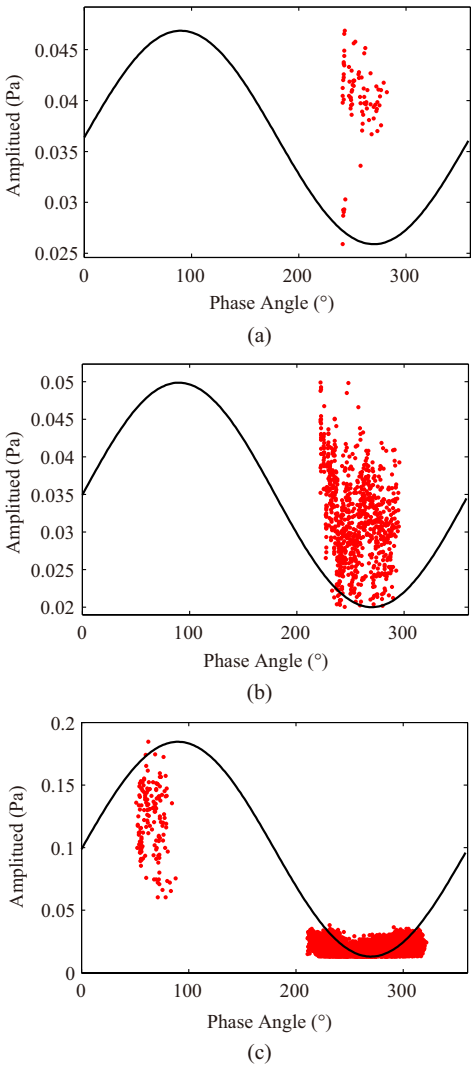

Fig. 8. Phase spectrum figures of pulse amplitudes from AC corona discharge. (a) 31.27 kV rms. (b) 38.16 kV rms. (c) 40.05 kV rms.

It can be seen from Fig. 8 that due to the random nature of the corona discharge, the pulse amplitudes locate at a large range of phase of the AC voltage. The sound pressure pulse first occurs at the negative half cycle and before the negative peak of the AC voltage. With the increase of the applied voltage, the phase angle gradually extends to larger ranges and pulse numbers increase. The onset voltage of sound pressure pulses at positive half cycle is higher than that at negative half cycle. At the same peak voltage, the pulse number at positive half cycle is far less than that at negative half cycle. Fig. 9 shows the statistical results of pulse amplitudes at AC positive and negative half cycles at different voltages. The average pulse amplitude at positive half cycle is about 2 to 3 times larger than that at negative half cycle. Compared with the pulse amplitude from the DC positive corona as shown in Fig. 7(a), the pulse amplitude at AC positive half cycle may be a little higher. This may account for the accumulated negative ions in the previous negative half cycle, which may enhance the discharge at AC positive half cycle.

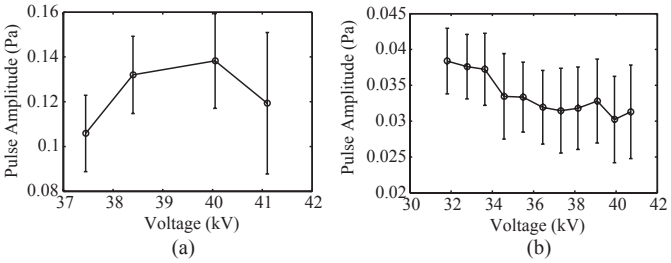

Fig. 9. Pulse amplitude varying with applied voltage at positive and negative half cycles. (a) Pulse amplitude at positive half cycle. (b) Pulse amplitude at negative half cycle.

Normally, the negative onset voltage is lower than the positive onset voltage. In the AC case, when the negative instantaneous voltage reaches the negative onset voltage, the negative corona discharge occurs. With an increase in applied voltage, the instantaneous voltage region that is higher than the onset voltage turns larger and thus the sound pressure pulses can be generated at a wider phase range. When the polarity of the voltage changes from negative to positive, the negative space charges are absorbed by the wire. The remaining negative space charges may accumulate around the corona source and hinder the increase in electric field at the streamer head, which may suppress the generation of positive streamer pulses. Thus, the onset voltage at positive half cycle is higher than that at negative half cycle.

The influence of the space charges on the corona discharge can be clearly seen from the pulse starting voltage and pulse ending voltage in the same half cycle. Fig. 10 shows the pulse starting and ending instantaneous voltages (denoted as U_{S} and U_{E} respectively) in negative half cycle varying with the RMS value of the AC voltage. The pulse starting voltage is lower than the pulse ending voltage. Moreover, the starting instantaneous voltage of sound pulse is approximately unchanged because the negative ions generated at negative half cycle are absorbed at positive half cycle; their influence on the onset corona at negative corona is very small. Once the corona occurs, the negative ions accumulate and suppress the occurrence of corona. With increased applied voltage, the suppression will become stronger, resulting in an increased ending instantaneous voltage.

D. Frequency Characteristics of AN

According to the time-domain waveform of AN, the frequency characteristics can be obtained on the basis of Fourier analysis. The typical waveform of single sound pressure pulse

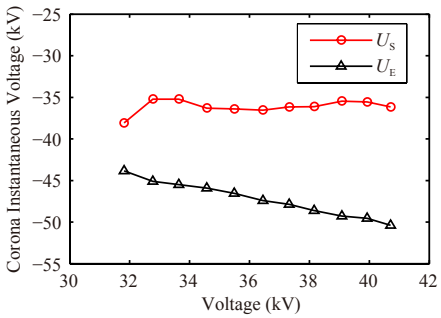

Fig. 10. Starting and ending instantaneous voltage of sound pressure pulses in negative cycle.

can be expressed as a segmented two exponential function and its Fourier transformation can be expressed in (4) [13].

$$P(\mathrm{j}\omega) = \int_{-\infty}^{\infty} p(t)\, e^{-\mathrm{j}\omega t} dt \tag{4}$$
$$= \frac{K_1 p_{\mathrm{m}1} e^{-\mathrm{j}\omega t_{\mathrm{p}0}}}{\alpha_1 - \mathrm{j}\omega} - \frac{K_1 p_{\mathrm{m}1} e^{-\alpha_1 t_{\mathrm{p}0}}}{\alpha_1 - \mathrm{j}\omega} - \frac{K_1 p_{\mathrm{m}1} e^{-\mathrm{j}\omega t_{\mathrm{p}0}}}{\beta_1 - \mathrm{j}\omega}$$
$$+ \frac{K_1 p_{\mathrm{m}1} e^{-\beta_1 t_{\mathrm{p}0}}}{\beta_1 - \mathrm{j}\omega} - \frac{K_2 p_{\mathrm{m}2} e^{-\mathrm{j}\omega t_{\mathrm{p}0}}}{\alpha_2 - \mathrm{j}\omega} + \frac{K_2 p_{\mathrm{m}2} e^{-\mathrm{j}\omega t_{\mathrm{p}0}}}{\beta_2 - \mathrm{j}\omega}$$

where $p_{\mathrm{m}1}$ and $p_{\mathrm{m}2}$ are the pulse amplitudes of the positive sound pressure part and the negative pressure part, respectively. The amplitude frequency spectrums of the single sound pressure pulses from DC and AC corona are shown in Fig. 11, and the corresponding time-domain waveforms are shown in Fig. 6. The frequency spectrum for the single sound pressure pulse under negative corona is smaller than that under DC positive corona. Similar results can be found between the AC positive and negative half cycles.

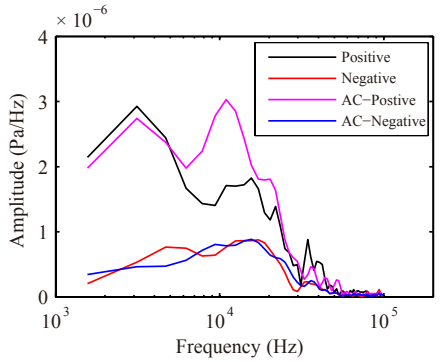

Fig. 11. Amplitude frequency spectrums of single sound pressure pulse.

The corona-generated AN consists of a series of sound pressure pulses with random time interval. With the help of the frequency spectrum of single sound pressure pulse, the frequency spectrum of the long-time measured AN can be expressed as

$$P_{\mathrm{train}}(\mathrm{j}\omega) = \sum_{i=1}^{N} P_i(\mathrm{j}\omega) \exp\left(-\mathrm{j}\omega \sum_{m=1}^{i-1} T_{\mathrm{I}}(m)\right) \tag{5}$$

where $P_i(\mathrm{j}\omega)$ is the frequency spectrum of the i^{th} sound pressure pulse, T_{I} is the time interval of the sound pressure pulse, and N is the pulse number in the time-domain waveform. In fact, the amplitude of the sound pressure pulse from corona discharge is small, and thus the linearized assumption for the sound pressure can be approximately reasonable for the weak ionization of the corona discharge [13]. Therefore, the frequency spectrum from a single corona source can be expressed as the sum of the frequency spectrums of all sound pressure pulses with shift of phase, as shown in (5).

Fig. 12 gives the amplitude frequency spectrums for the AN from DC and AC corona discharge. It should be pointed out that the sound pressure pulses under the selected DC applied voltages are not too dense, indicating the corona discharge is not intense. And the pulse rates for DC positive and negative applied voltages are at the same order of magnitude. While the AC applied voltage is selected to insure the sound pressure pulses exist at both the positive and negative half cycles.

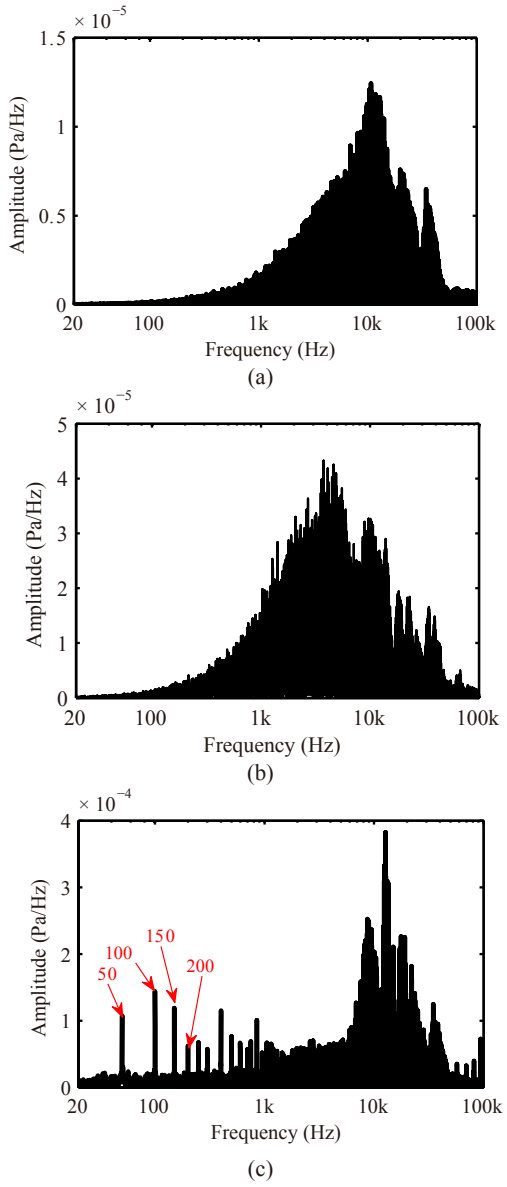

Fig. 12. The frequency spectrum of the AN from DC and AC corona discharge. (a) DC negative corona at −48 kV. (b) DC positive corona at 56 kV. (c) AC corona at 40.05 kVrms.

For the DC corona-generated AN, the frequency spectrum covers wide range of frequencies and the high frequency components whose frequencies are higher than 1 kHz are notable. The peak value of the frequency spectrum under DC negative voltage tends to higher frequencies compared with that under DC positive voltage. But most of components of its amplitude frequency spectrum are smaller than those under DC positive voltage. In fact, considering the function of A-weighted network, the frequency components above 1 kHz give the most contribution on the A-weighted sound pressure level which is commonly used as the evaluation indicator of noise level [25], [26]. Therefore, the positive corona is the main source of the AN based on the higher amplitudes of frequency spectrum and sound pressure pulses.

For the AC corona-generated AN, the frequency spectrum in Fig. 12(c) shows marked differences from that under DC corona discharge. There are some pure tones at frequencies of the harmonics of 50 Hz power frequency, which are induced by the modulation of the alternating voltage of the pulse trains. And the high frequency components reflect the sound pressure pulses at each half cycle of AC voltage. In addition, the AN from AC corona discharge seems to be higher than that from DC corona discharge, which is consistent with the previous statistical results from the transmission lines [1] and is similar to the results of electromagnetic interference caused by corona current pulses [20].

IV. Conclusions

This paper presents experimental investigations on the AC and DC corona-generated audible noise. The comparisons of the time-domain detail characteristics of sound pressure pulse and frequency spectrum are given.

A de-noising method for the audible noise from single corona source is proposed on the basis of the correlation analysis and the sound pressure pulse characteristics. Through the de-noising method, the sound pressure pulses from DC and AC corona can be successfully extracted and the influence of the background noise can be removed.

The waveform of AN from DC positive corona has larger pulse amplitude, less pulse number, and larger randomness compared with that from DC negative corona. For the AC corona, the sound pressure pulse first occurs at the negative half cycle. The onset voltage of sound pressure pulses at positive half cycle is higher than that at negative half cycle. At the same peak voltage, the pulse number at positive half cycle is far less than that at negative half cycle. This may be due to the influence of the space charges.

In frequency domain, the peak value of the frequency spectrum under DC negative voltage tends towards higher frequencies compared with that under DC positive voltage. However, most components of its amplitude frequency spectrum are smaller than those under DC positive voltage. The AN from AC corona has typical pure tones caused by the modulation of alternating voltage and has higher noise level than that under DC corona.

References

[1] P. S. Maruvade, *Corona in Transmission Systems: Theory, Design and Performance*. Johannesburg, South Africa: Eskom Holdings, 2011, 260–272, 372–376.

[2] R. J. Lings, "Audible noise," in *EPRI AC Transmission Line Reference Book—200 kV and Above*, 3rd ed. Palo Alto, CA: Electric Power Research Institute, 2005, ch. 10, pp. 10, 1–49.

[3] N. Yukio and S. Yoshitaka "Availability of corona cage for predicting audible noise generated from HVDC transmission line," *IEEE Transactions on Power Delivery*, vol. 4, no. 2, pp. 1422–1431, 1989.

[4] V. L. Chartier, and R. D. Stearns, "Formulas for predicting audible noise from overhead high voltage AC and DC lines," *IEEE Transactions on Power Apparatus and Systems*, vol. 100, no. 1, pp. 121–130, 1981.

[5] A. C. Baker, M. G. Comber, and K. E. Ottosen, "Investigations of the corona performance of conductor bundles for 800 kV transmission lines," *IEEE Transactions on Power Apparatus and Systems*, vol. 94, no. 4, pp. 1117–1130, 1975.

[6] F. Ianna, G. L. Wilson, D. J. Bosack, "Spectral characteristics of acoustic noise from metallic protrusions and water droplets in high electric fields," *IEEE Transactions on Power Apparatus and Systems*, vol. PAS-93, no. 6, pp. 1787–1796, 1974.

[7] K. H. Yang, D. I. Lee, G. H. Hwang, J. H. Park, and V. L. Chartier, "New formulas for predicting audible noise from overhead HVAC lines using evolutionary computations," *IEEE Transactions on Power Delivery*, vol. 15, no. 4, pp. 1243–1251, Oct. 2000.

[8] Z. Engel and T. Wszolek, "Audible noise of transmission lines caused by the corona effect: analysis, modeling, prediction," *Applied Acoustics*, vol. 47, no. 2, pp. 149–163, 1996.

[9] M. Sforzini, R. Cortina, G. Sacerdote, and R. Piazza, "Acoustic noise caused by AC corona on conductors: results of an experiment investigation in the anechoic chamber," *IEEE Transactions on Power Apparatus and Systems*, vol. PAS-94, no. 2, pp. 591–601, 1975.

[10] D. E. Perry, "An analysis of transmission line audible noise levels based upon field and three-phase test line measurements," *IEEE Transactions on Power Apparatus and Systems*, vol. PAS-91, no. 3, pp. 857–865, 1972.

[11] X. M. Bian, L. Chen, D. M. Yu, J. M. K. MacAlpine, L. M. Wang, and Z. C. Guan, "Influence of aged conductor surface conditions on AC corona-generated audible noise with a corona cage," *IEEE Transactions on Dielectrics and Electrical Insulation*, vol. 19, no. 6, pp. 2037–2043, 2012.

[12] P. Heroux and N. G. Trinh, "A statistical study of electrical and acoustical characteristics of pulsative corona," in *IEEE PES Winter Meeting*, New York, 1976, pp. 760.

[13] X. B. Li, X. Cui, T. B. Lu, D. Zhang, and Y. Liu, "Time-domain characteristics of the audible noise generated by single corona source under positive voltage," *IEEE Transactions on Dielectrics and Electrical Insulation*, vol. 22, no. 2, pp. 870–878, Apr. 2015.

[14] X. B Li, X. Cui, T. B. Lu, Y. Liu, D. Zhang, and Z. G. Wang, "The correlation between audible noise and corona current in time domain caused by single positive corona source on the conductor," *IEEE Transactions on Dielectrics and Electrical Insulation*, vol. 22, no. 2, pp. 1314–1320, Apr. 2015.

[15] F. Bastien, "Acoustics and gas discharge: applications to loudspeakers," *Journal of Physics D: Applied Physics*, vol. 20, no. 12, pp. 1547–1557, 1987.

[16] Ph. Bequin, V. Montembault, and Ph. Herzog, "Modelling of negative point-to-plane corona loudspeaker," *The European Physical Journal: Applied Physics*, vol. 15, no. 1, pp. 57–67, 2001.

[17] U. Straumann, "Simulation of the space charge near coronating conductors of AC overhead transmission lines," *Journal of Physics D: Applied Phys*ics, vol. 44, no. 7, pp. 075502: 1–9 2011.

[18] U. Straumann, "Mechanism of the tonal emission from AC high voltage overhead transmission lines," *Journal of Physics D: Applied Physics*, vol. 44, no. 7, pp. 075501: 1–8, 2011.

[19] X. B. Li, X. Cui, T. B. Lu, D. Zhang, Z. G. Wang, and W. Z. Ma, "Time-domain and frequency domain characteristics of audible noise from single corona source," in *2014 International Conference on Power System Technology*, Sichuan, China, pp. 1410–1416, 2014.

[20] S. Zhang, B. Zhang, and J. L. He, "Comparison of direct current and 50 Hz alternating current microscopic corona characteristics on conductors," *Physics of Plasmas*, vol. 21, no. 6, pp. 063503, 2014.

[21] G. W. Trichel, "The mechanism of the negative point to plane corona near onset," *Physical Review*, vol. 54, no. 12, pp. 1078–1084, 1938.

[22] D. D. Hinde, "Corona discharges on the surface of high voltage composite insulators," Ph. D. dissertation, Queensland University of Technology, Brisbane, Australia, 2009.
[23] R. E. Klinkowstein, "A study of acoustic radiation from electrical spark discharge in air," M. S. thesis, Massachusetts Institute of technology, Cambridge, MA, 1974.
[24] Y. C. Cheng, C. R. Li, and X. Q. Huang, "Study of corona discharge pattern on high voltage transmission lines for inspecting faulty porcelain insulators," *IEEE Transactions on Power Delivery,* vol. 23, no. 2, pp. 945–952, Apr. 2008.
[25] Q. Li, R. Shuttleworth, G. Zhang, I. Dupere, and S. M. Rowland, "Acoustic noise evaluation for overhead line conductors," in *2013 Electrical Insulation Conference*, Ottawa, Canada, June 2013, pp. 119-123.
[26] *IEEE Standard for the Measurement of Audible Noise from Overhead Transmission Lines*. IEEE Standard 656-1992.

Xuebao Li (S'13) was born in Tianjin, China, in 1988. He received the B.Sc. degree in electrical engineering in North China Electric Power University, Beijing, China, in 2011, where he is currently pursuing the Ph.D. degree. His main research interest is electromagnetic compatibility in power systems.

Xiang Cui (M'97–SM'98) was born in Baoding, Hebei Province, China, in 1960. He received the B.Sc. and M.Sc. degrees in electrical engineering from North China Electric Power University, Baoding, in 1982 and 1984, respectively, and the Ph.D. degree in accelerator physics from China Institute of Atomic Energy, Beijing, China, in 1988. He is currently a Professor and the Head of the Electromagnetic and Applied Superconductivity Laboratory, North China Electric Power University. His research interests include computational electromagnetics, electromagnetic environment and electromagnetic compatibility in power systems, insulation, and magnetic problems in high-voltage apparatus. Prof. Cui is an Associate Editor of IEEE Transactions on Electromagnetic Compatibility and a member of the editorial advisory board of the International Journal for Computation and Mathematics in Electrical and Electronic Engineering.

Tiebing Lu was born in Hebei Province, China, in 1970. He received the B.Sc. and M.Sc. degrees in electronic engineering from Xi'an Jiaotong University in 1991 and 1994, respectively, and the Ph.D. degree in electrical engineering from North China Electric Power University in 2002, Baoding, China. He is currently a Professor in the School of Electrical and Electronic Engineering, North China Electric Power University. His research interests are electromagnetic compatibility in power systems and the numerical methods of the electromagnetic fields.

Donglai Wang was born in Shenyang, Liaoning Province, China, in 1991. He received the B.E. degree in electrical engineering in North China Electric Power University, Beijing, China, in 2013, where he is currently pursuing the Ph.D. degree. His main research interest is electromagnetic compatibility in power systems.

Wenzuo Ma was born in Hebei Province, China, in 1991. He received the B.Sc. degree in electrical engineering in Shi Jiazhuang Railway University. He is currently pursuing the M.Sc. degree in North China Electric Power University.

Xingming Bian was born in Jiangsu Province, China, in 1985. He received the B.S. degree in electrical engineering from Huazhong University of Science and Technology, Wuhan, China, in 2006. He received the Ph.D. degree in electrical engineering at Tsinghua University in 2012, Beijing, China. He is currently an Associate Professor in the School of Electrical and Electronic Engineering, North China Electric Power University. His research interests are in electromagnetic environment of power systems, and high voltage insulation and optimization of grading rings of insulators in power system.